

# Supporting Information

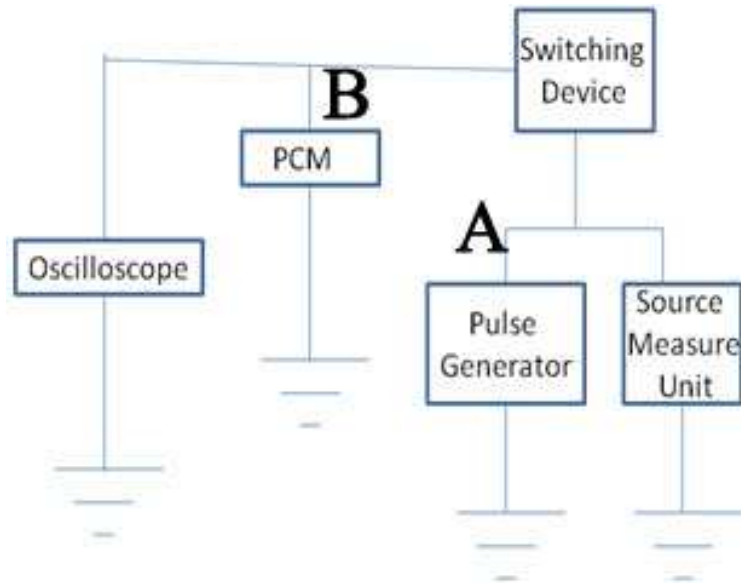
## Ti-Sb-Te Alloy: A Candidate for Fast and Long-Life Phase-Change Memory

Mengjiao Xia,<sup>1,2</sup> Min Zhu,<sup>1,\*</sup> Yuchan Wang,<sup>1,2</sup> Zhitang Song,<sup>1</sup> Feng Rao,<sup>1</sup> Liangcai Wu,<sup>1</sup> Yan Cheng<sup>1</sup> and Sannian Song<sup>1</sup>

<sup>1</sup>*State Key Laboratory of Functional Materials for Informatics, Laboratory of Nanotechnology, Shanghai Institute of Micro-System and Information Technology, Chinese Academy of Sciences, Shanghai 200050, People's Republic of China*

<sup>2</sup>*University of the Chinese Academy of Sciences, Beijing 100080, People's Republic of China*

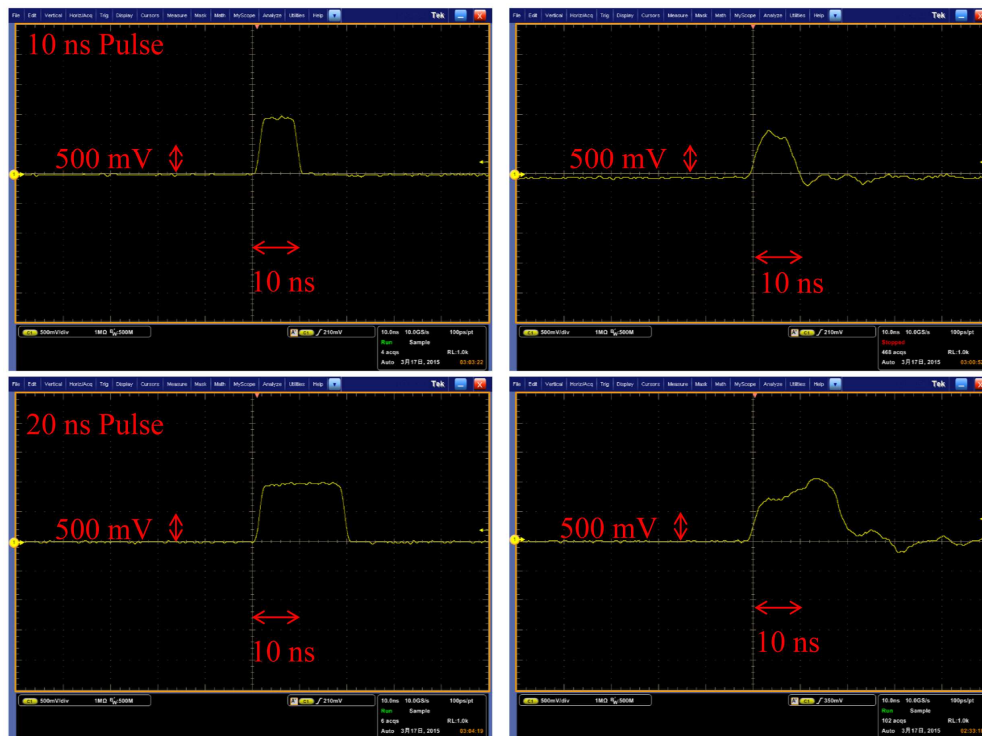
\*E-mail: minzhu@mail.sim.ac.cn



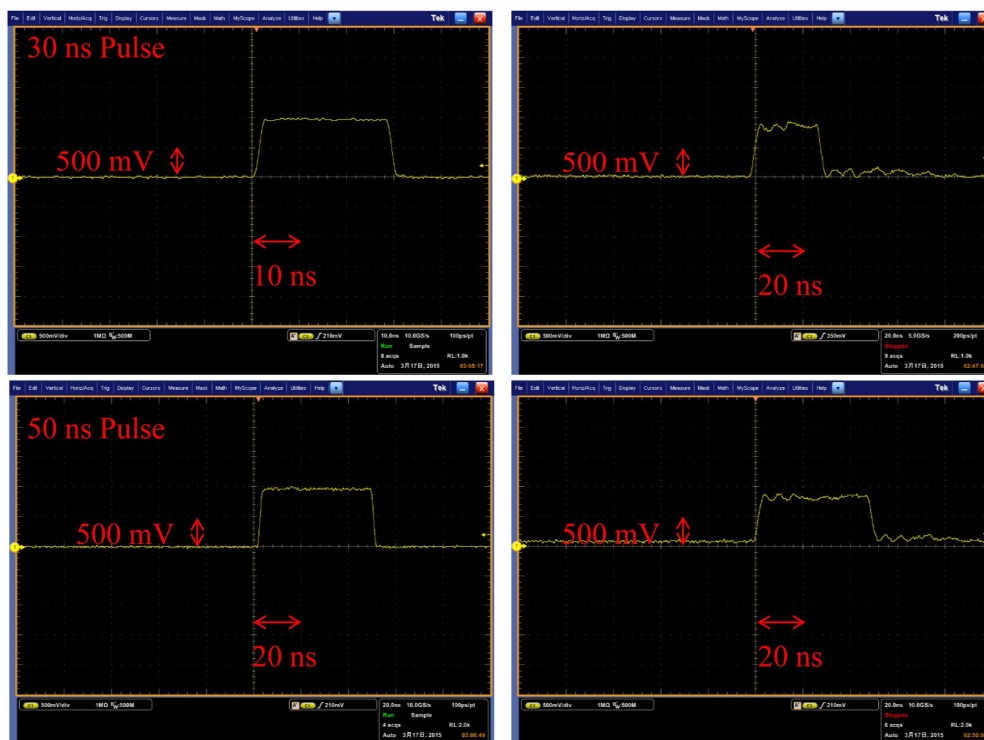
**Figure S1** Schematic picture of the electrical test setup

Figure S1 shows the schematic picture of our electrical test setup. First, we monitored the voltage pulses from the pulse generator (point A, Figure S2-S5). The amplitude, rising and falling slopes of the pulse is set to 1 V/2 ns/2 ns. From these figures, we can see that all the waveforms of pulses at point A are very close to the idea ones. In the experiments, the full widths at half maximum (FWHM) values of the pulses were used to characterize the switching speeds of the cells.

However, provided a 10 ns or 20 ns width pulse, the monitored pulses at point B become somewhat distorted, including amplitude and width (Figure S2). Besides, there are many sub-pulses after the major pulse, which may influence the device performance. As the increase of the provided pulse width, the waveform gets much better (Figure S3-S5).



**Figure S2** Monitored voltage pulses with 10 ns (top) and 20 ns (bottom) widths at point A (left) and B (right).



**Figure S3** Monitored voltage pulses with 30 ns (top) and 50 ns (bottom) widths at point A (left) and B (right).

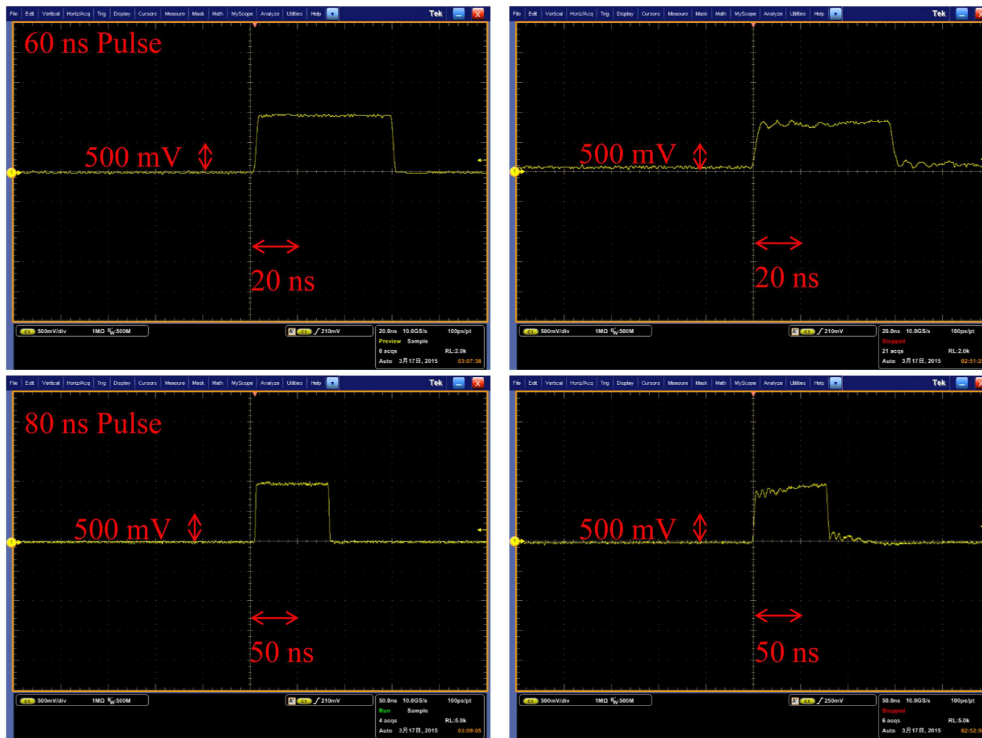


**Figure S4** Monitored voltage pulses with 60 ns (top) and 80 ns (bottom) widths at point A (left) and B (right).

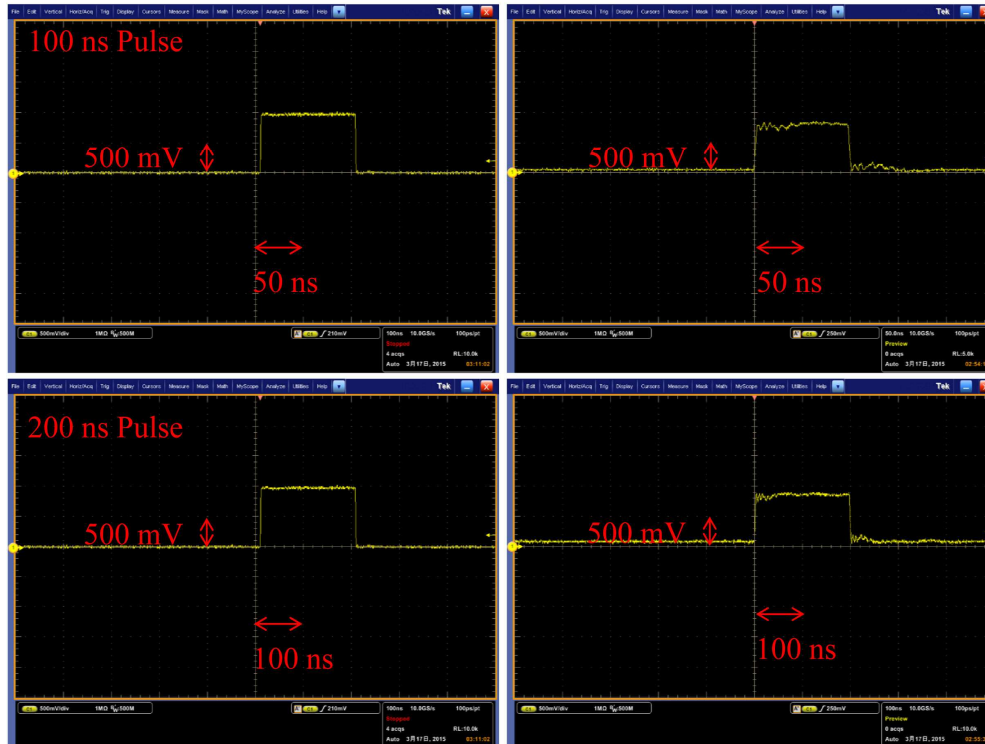


**Figure S5** Monitored voltage pulses with 100 ns (top) and 200 ns (bottom) widths at point A (left) and B (right).

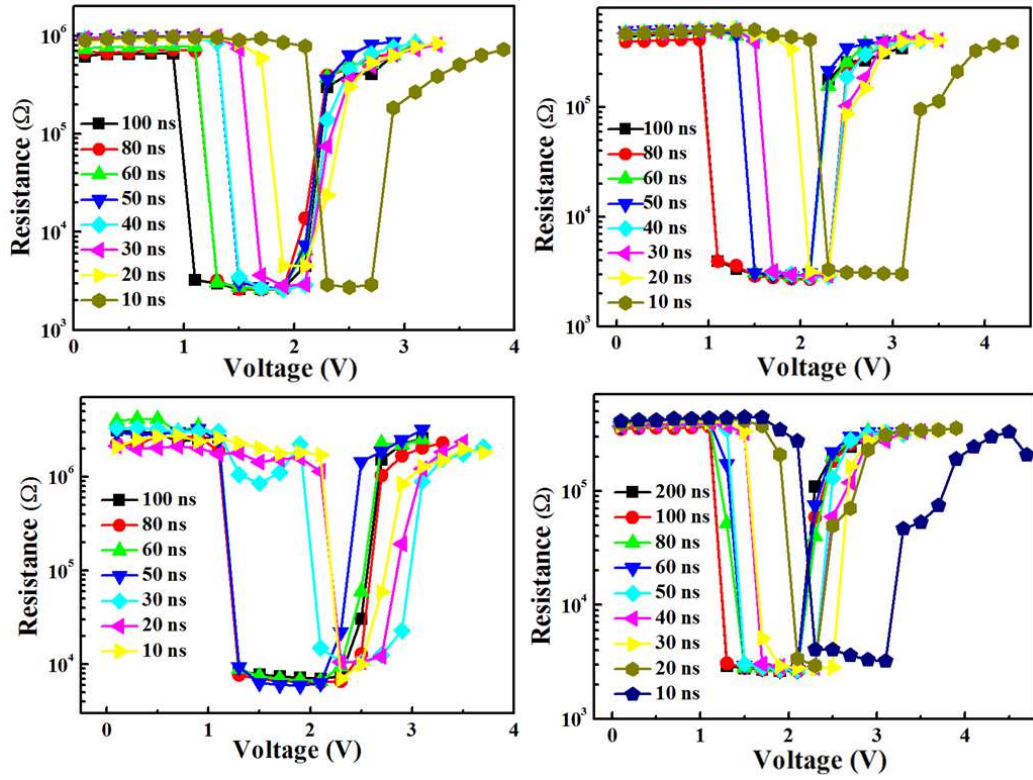
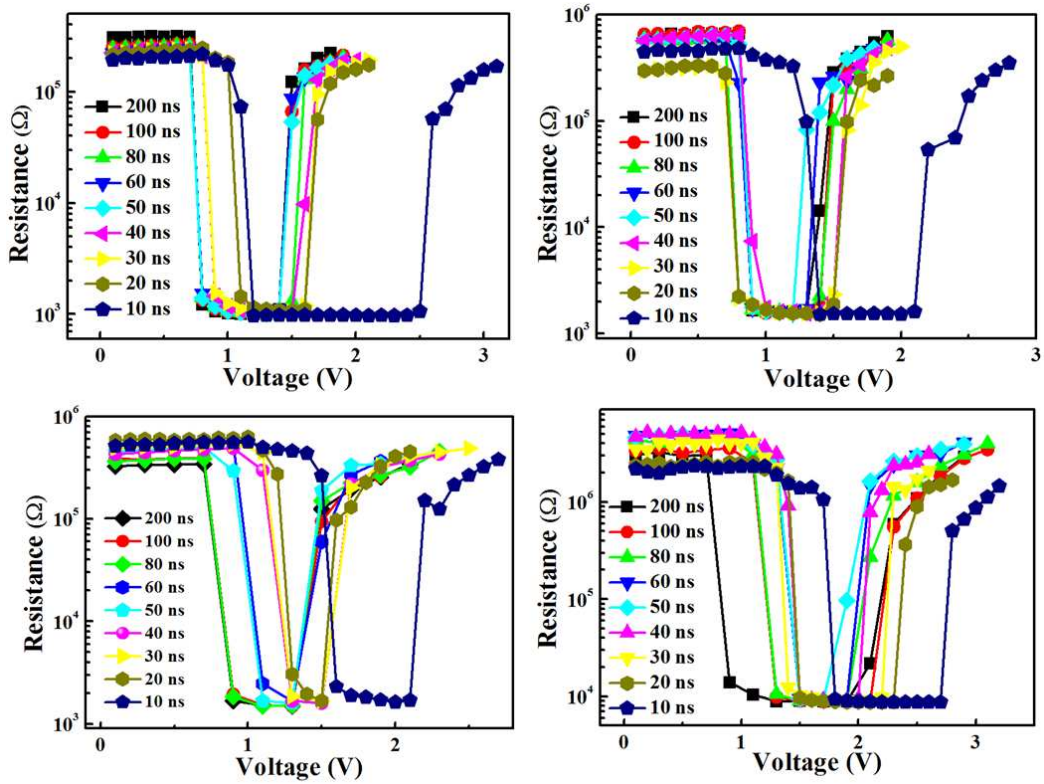
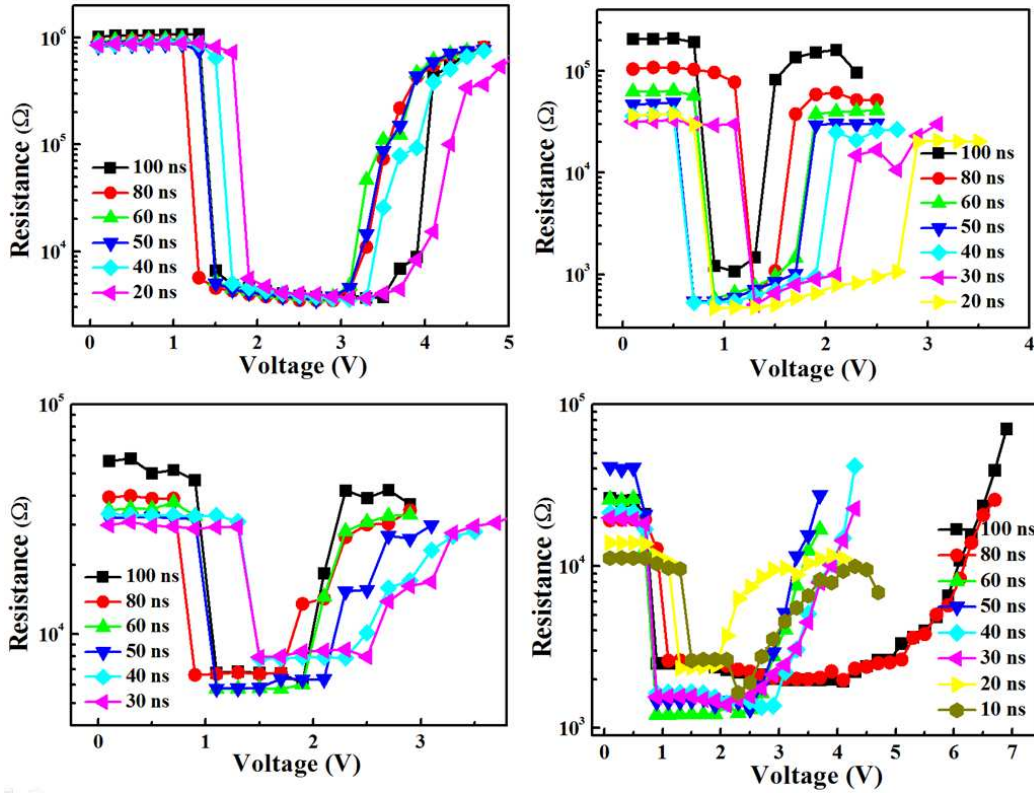


Figure S6 Resistance-voltage curves for other  $Ti_{0.32}ST$ -based PCM cells in the device array.



**Figure S7** Resistance-voltage curves for other  $Ti_{0.43}ST$ -based PCM cells in the device array.



**Figure S8** Resistance-voltage curves for other  $Ti_{0.56}ST$ -based PCM cells in the device array.

Figure S6-S8 show the resistance-voltage results of other cells in the  $Ti_{0.32}ST$ ,  $Ti_{0.43}ST$ , and  $Ti_{0.56}ST$ -based PCM device array, respectively. We can see that the required operation voltages for  $Ti_{0.32}ST$  and  $Ti_{0.43}ST$ -based PCM cells are very uniform. The high resistance and low resistance fluctuate within one order of magnitude, which are in the normal resistance distributions for PCM devices (H. Y. Cheng et al. IEDM, 2013, pp.30.6.1-30.6.4). However, as shown in Figure S6, the uniformity of  $Ti_{0.56}ST$ -based PCM cells is much worse either in resistance or operation voltages. The inhomogeneous phase of  $Ti_{0.56}ST$  after repeated operations is the possible reason for the bad uniformity.